Applied Physics B (2023) 129:90
https://doi.org/10.1007/s00340-023-08036-5

Applied Physics B
Lasers and Optics

RESEARCH

Spectral investigation of soot absorption properties during laser-induced incandescence measurements

Francesca Migliorini[1] · Roberto Dondè[1] · Silvana De Iuliis[1]

Received: 28 February 2023 / Accepted: 2 May 2023

Abstract
The effect of rapid laser irradiation on the optical properties of mature soot particles is investigated by performing wavelength-resolved extinction measurements in the visible spectral region. In particular, the spectral behavior of the absorption properties is explored during laser irradiation, at the peak of the incandescence signal (prompt LII) and few nanoseconds after the peak, and finally when particles have reached an equilibrium condition with the surrounding gas. A significant variation of the absorption coefficient of the laser-irradiated soot particles compared to that of the pristine ones is observed already at the LII peak. Such variation keeps evolving with time until it reaches a final permanent value. Results are presented in relation to the laser fluence used for irradiation and discussed with the aim of stressing the need of knowing the entity of the modification of soot absorption properties during laser irradiation for a correct interpretation of LII data.

1 Introduction

Laser-induced incandescence (LII) is nowadays a widely used diagnostic tool for in-situ soot characterization (volume fraction and soot primary particles size) in combustion and ambient atmospheric environments [1] thanks to its high sensitivity and species selectivity.

In the last decades, the strong interest in understanding the physics at the basis of the technique led to the evidence that intense laser irradiation produces effects on particles internal structure [2–4], induces sublimation and loss of material from soot particles and also promotes the formation of new particles as a result of vaporization effects [5, 6]. In turn, these phenomena affect the optical properties of the particles under investigation as highlighted by several studies on the effect of laser irradiation on soot optical properties in relation to soot maturity, the degree of the heating process as well as the measurements integration time [6–11]. However, the overall picture is still not clear so that the interpretation of the LII signal is usually performed assuming that soot optical properties are not affected by rapid laser heating, although a change in the absorption, scattering and incandescence properties during laser heating was observed. Moreover, LII itself is used to study the absorption properties of soot particles using two excitation wavelengths [12–15] without considering that during the irradiation process the absorption properties themselves might be altered to some extent.

The complexity of the issue lies in the limited knowledge on how the processes occurring during laser irradiation depend on the structure, morphology, composition and maturity degree of the particles under analysis. In a recent work, we performed double-pulsed LII experiments on soot particles sampled from a premixed flame and we observed that young and mature soot behave differently under laser irradiation [16, 17]. A strong enhancement of the absorption efficiency of young particles was observed already under low laser fluence irradiation resulting in an increase of both LII signal and temperature with respect to the corresponding non-irradiated particles. On the contrary, the absorption properties of mature soot particles appear not to be strongly affected by laser irradiation. Similar results were obtained also by Török et al. [18], who pre-heated different types of soot with a first laser pulse and used LII at two excitation wavelengths (532 and 1064 nm) to study the induced changes in the properties of young as well as mature soot by rapid laser heating. They observed that pre-heated young soot exhibits an enhancement of both the absorption efficiency of soot and the peak LII intensity already for modest pre-heating while for mature soot the absorption enhancement

✉ Francesca Migliorini
francesca.migliorini@cnr.it

[1] ICMATE-CNR, Institute of Condensed Matter Chemistry and Technologies for Energy, Via R. Cozzi 53, 20125 Milan, Italy

Published online: 12 May 2023

was probably due to particles annealing and prominent mass loss was also observed. Despite these recent findings, more work is still needed to assess the impact of laser irradiation on the absorption properties of different types of soot particles and thus the effect on the interpretation of laser diagnostics.

The present work explores further the issue of the absorption properties of laser-irradiated particles by investigating, for the first time, the time-evolution of the spectral behavior of soot absorption properties during laser irradiation. To this purpose, particular effort has been made to develop a new experimental setup suitable for the investigation of the particles absorption properties during LII measurements. In particular, extinction measurements are carried out at the "prompt" LII signal [19] (defined as the integral over a gate width of 4 ns, 1 ns before and 3 ns after the peak), few nanoseconds after the LII peak and when particles are cooled down to the surrounding environment temperature.

The results obtained in this work prove the change of the absorption properties already during the laser pulse and highlight the need of taking into account such variation for a correct interpretation of LII data or at least among the uncertainties of the measurement.

2 Experimental setup and methodology

Soot nanoparticles are produced by a nitrogen-quenched ethylene diffusion flame in air at atmospheric pressure. The hydrocarbon fuel, the fuel flow rate (visible flame height) and the quenching height are chosen to obtain mature soot particles. The SEM image reported as insert (a) in Fig. 1 shows an example of the sampled soot particles. More details on soot particles production can be found in our previous work [6]. After being probed in the exhaust plume, soot particles flow in a tube where they are irradiated by a high-power laser pulse of few nanosecond duration (Nd:YAG laser, 7.9 ns duration, top-hat profile). The sampling flow, the length of the irradiation tube and the laser frequency are adjusted to ensure that the sampled particles are heated only by a single laser pulse [6]. The laser energy density is varied in the range 0–400 mJ cm^{-2}.

Extinction measurements on pristine and laser-irradiated particles are carried out in the visible spectral region. To perform these measurements during and after laser irradiation, two different experimental setups are arranged. For simplicity, from now on, we refer to these two measurement conditions as *LII peak* and *final*, respectively.

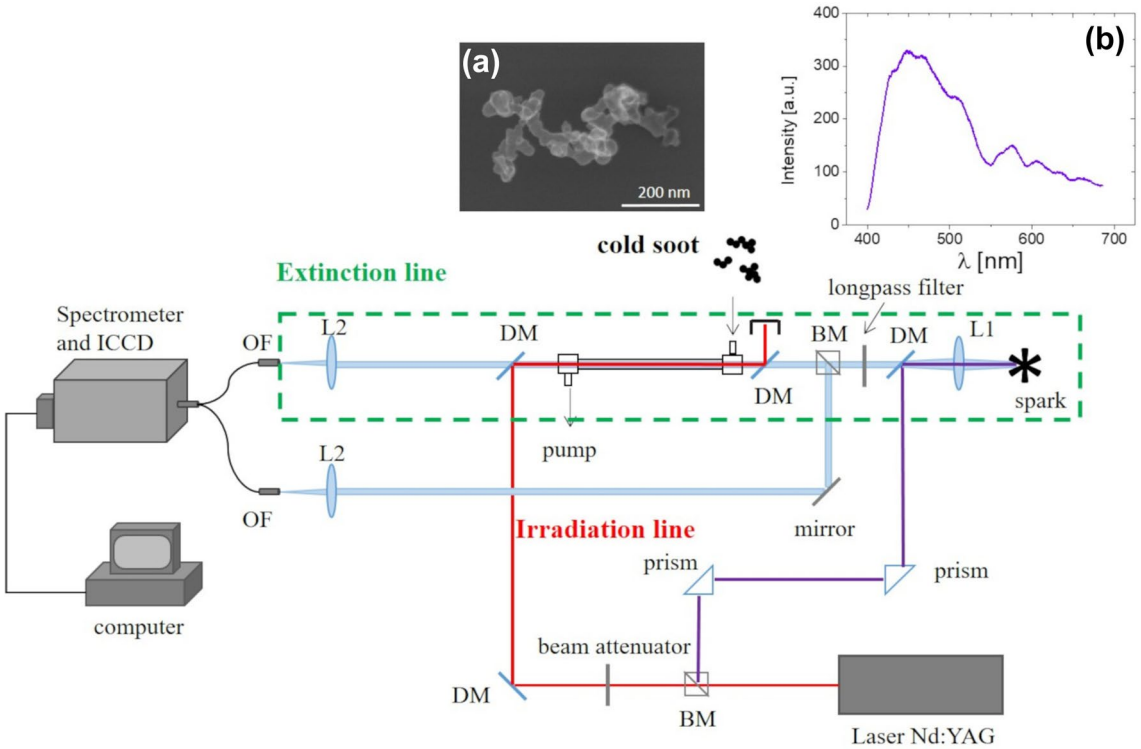

Fig. 1 *LII peak* experimental setup. The red line represents the portion of the IR laser beam used for heating the particles, while the purple line represents the portion used for generating the spark. The optical path used for the extinction measurements is highlighted with a green rectangle. The optical elements used are the following: beam splitters (BM), prisms, dichroic mirrors (DM), lenses (L1 and L2) and optical fibers (OF). Inserts: SEM image of sampled particles (**a**) and spark spectrum (**b**)

The *final* experimental setup is similar to the one presented in Fig. 1 in Migliorini et al. [6] and here only briefly recalled. It consists of two 20-cm-long glass tubes equipped with quartz windows at the extremities. Cold soot particles are pumped into the first tube (irradiating tube) where they are heated by a single laser pulse. After laser irradiation, soot particles flow into the second tube (measuring tube) where extinction measurements are performed. An intense diffuse light produced by a Halogen lamp (36 V, 400 W) is collimated through the measuring tube and imaged onto an optical quartz fiber (Oriel, 3 mm bundle diameter) coupled with a Czerny-Turner spectrograph (Shamrock 303i) connected to an ICCD camera (iStar 334 T, Andor Technology).

The experimental setup for *LII peak* measurements is shown in Fig. 1. Since extinction measurements are carried out during laser irradiation, only one tube is needed. Nevertheless, due to the very short measurement time, namely 4 ns (at the LII prompt incandescence signal), the intensity of the Halogen lamp is comparable to the intensity of the LII signal, resulting in a strong influence on the transmissivity measurements. For this reason, in the literature the investigation of the absorption properties of laser-heated soot is performed with lasers as light sources thus limiting the investigation to defined wavelengths [7, 8, 11].

To overcome this problem and reduce the contribution of the incandescence signal to the transmitted intensity, a more powerful light source is used for extinction measurements. This light source consists in a spark generated by the interaction of the laser beam on a copper target, similarly to the method developed by Borghese et al. [20]. In particular, the IR laser beam used for irradiation is split into two paths by means of a beam splitter (25/75%). One portion is used for particles heating in the irradiation/measuring tube (75%) and the other one is used to produce a spark (25%), focalizing the beam on the target by means of a 115 mm focal length lens (L1). A beam attenuator is placed before the first dichroic mirror to change the energy density of the laser. The spectrum of such a pulsed source, reported in the insert (b) in Fig. 1, is characterized by a broadband emission (400–700 nm) of about 30 ns duration due to Bremsstrahlung radiation. To perform extinction measurements, the beam obtained by the collimated spark light is split into two paths by means of a beam splitter (25/75%): the primary optical path (75%) passing through the irradiation/measuring tube, while the secondary optical path (25%), bypassing the tube, is used as a reference to correct for the shot-to-shot spark intensity variation.

The transmitted and reference signals are then focused onto two 1-mm-optical fibers with two 100-mm focal length lens, L2. The two fibers are coupled so that the two beams are shifted vertically onto the entrance slit of the spectrograph, ensuring that the signals (i.e., incident or transmitted light) and the reference are collected at the same time. In this way, any variation in the spark intensity during the acquisition period is captured.

In both configurations, *final* and *LII peak*, the spectrograph is configured to measure in the wavelength range from 400 to 685 nm. This range is selected to cover the same spectral region with both the lamp and the spark. A long-pass filter at 395 nm is placed in front of the light sources to avoid second-order effects**.** For these measurements, the low resolution grating (150 grooves/mm) is used, resulting in 0.28 nm spectral resolution. The integration time for all the measurements with the *LII peak* setup is set to 4 ns while it is 1 µs for the *final* condition.

We briefly recall that the extinction of light can be generally described by the Beer–Lambert law:

$$\tau_\lambda = \frac{I_{\lambda,T}}{I_{\lambda,0}} = \exp\left(-\int_0^L k_{\mathrm{ext}(\lambda)}\mathrm{d}x\right), \tag{1}$$

where τ_λ is the transmissivity, $I_{\lambda,T}$ is the transmitted light, $I_{\lambda,0}$ is the incident light, $k_{\mathrm{ext}(\lambda)}$ the extinction coefficient of the dispersed particles at a certain wavelength and x is the spatial location along the path. If the distribution of particles in the medium is uniform along the line-of sight, Eq. 1 simplifies to

$$-\ln\tau_\lambda = k_{\mathrm{ext}(\lambda)}L, \tag{2}$$

where L is the length of the light path through the medium.

Measurements of incident and transmitted light are carried out with different procedures in the case of *final* and *LII peak* measurements. For the *final* measurements, the spectrograph is set to the full vertical binning mode and the incident and the transmitted light spectra are collected sequentially, as an average of 300 spectra each. Then the transmissivity is obtained by the ratio of the transmitted and the incident spectra, both background-corrected. For the *LII peak* measurements, as the measure and reference signals are simultaneously focused onto the entrance slit, the spectrograph is set to the image mode. A typical image is shown in Fig. 2 where the horizontal axis of each image is the spectral axis.

The top of each image represents the spectrum related to the primary optical path (i.e. the light passing through the tube) and the bottom part is the spectrum of the secondary optical path which is the reference signal. Each image consists of 300 acquisitions for each measurement (i.e., incident and transmitted light). The data used for calculations are vertically integrated over the height of each spectrum (130 pixels) to reduce noise.

To take into account possible variations in the spark intensity and since the two optical paths do not necessarily

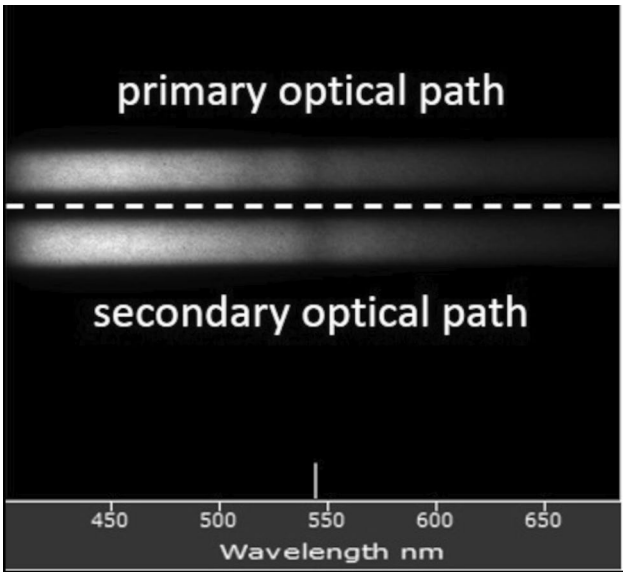

Fig. 2 Typical raw image of the *LII peak* measurements

have identical light transmission efficiencies, for each image, the primary optical path spectrum is divided by the secondary optical path. Finally, the transmissivity is obtained by the ratio between the reference-corrected transmitted and incident light signals. In section S1 in the Supplementary Material, we report the uncertainties related to both *LII peak* and *final* measurements.

3 Results and discussion

The spectral behavior of the extinction coefficient for pristine and laser-irradiated soot nanoparticles at different laser fluences (130, 260 and 400 mJ cm^{-2}) is investigated and shown in Fig. 3. The curves are normalized to average value of 1 at the upper wavelengths (660–680 nm) to account for a possible variation in particles concentration. The wavelength range for normalization is chosen considering that the extinction curves show a weaker spectral dependence at the longer wavelengths as also reported in the literature [6, 21–24]. The uncertainty associated with the extinction coefficient measurements is about 3% and is reported in Fig. 3 as grey shaded band. A variation of the extinction coefficient of the irradiated soot nanoparticles compared to the pristine ones can be observed already at 130 mJ cm^{-2}. In particular, while above 600 nm the spectra are quite overlapped, at shorter wavelengths a different trend of the extinction coefficient is detected for the irradiated soot already at the *LII peak* and the variation becomes more significant at the *final* measurement condition.

The trend looks more relevant increasing the energy density of the laser, suggesting that the phenomena

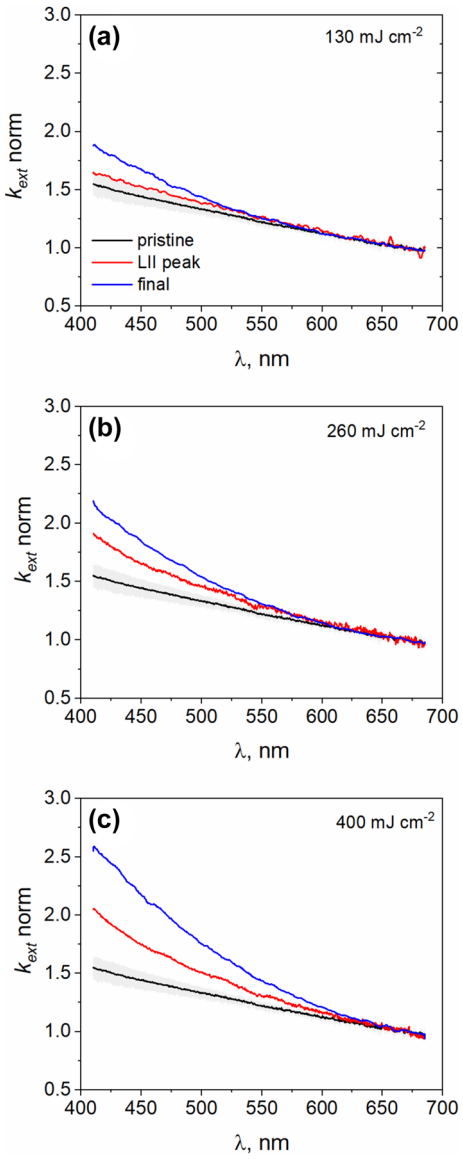

Fig. 3 Extinction coefficient spectral behavior of pristine and laser-irradiated particles for *LII peak* and *final* measurements at 130 mJ cm^{-2} (**a**), 260 mJ cm^{-2} (**b**), 400 mJ cm^{-2} (**c**). Data are normalized at the upper wavelengths (660–680 nm). The grey shaded band represents the uncertainty

happening during the interaction between the particles and the laser pulse strongly depends on the laser fluence. Such dependence is detected even if the particle temperature at 260 and 400 mJ cm^{-2} is almost the same, as we will show later in the text.

Therefore, laser irradiation seems to promote a permanent change in soot optical properties, in contrast with Thomson et al. [7], who observed a reversible modification of the extinction coefficient at 405 and 830 nm during the heating period. Only a small permanent increase of the refractive

index absorption function at 830 nm was observed, likely related to soot graphitization.

To better appreciate the difference in the extinction coefficient curves with laser fluence conditions, the k_{ext} spectra are fitted by a power-law function in the range 410–685 nm to retrieve the dispersion coefficient, α, which is widely used in the literature to assess the wavelength dependence of soot optical properties [25, 26]. In particular, the α values obtained for all the curves are normalized to the α value of the pristine particles.

Figure 4 shows the variation of the dispersion coefficient with laser fluence for the *LII peak* and *final* measurements and the related uncertainties. A significant increase of α with laser fluence is observed, thus highlighting a change in the optical properties under laser irradiation.

It is important to recall here that the extinction coefficient is made by two contributions, namely absorption and scattering. If present, scattering is in general more significant at short wavelengths and thus might strongly contribute to the significant variation of the extinction coefficient observed in Fig. 3. In similar experimental conditions, Migliorini et al. [6] evaluated the single scattering albedo SSA (defined as scattering coefficient over extinction coefficient) at 470 nm for pristine and laser irradiated particles. It was found that pristine particles exhibit a SSA of about 0.28, while a reduction of the single-scattering albedo with laser fluence was detected for the laser-irradiated particles. These data are here used to estimate the scattering contribution to extinction, thus obtaining information on the effect of laser irradiation on the particle absorption properties, which are the ones directly involved in LII data interpretation.

In particular, the scattering contribution is evaluated starting from the data in Fig. 3. At each laser fluence, the spectral behavior of the scattering coefficient is obtained from the SSA at 470 nm from Fig. 3 in Migliorini et al. [6], assuming a wavelength dependence of λ^{-2} according to

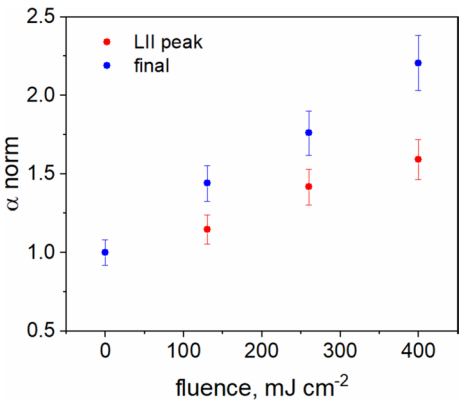

Fig. 4 Normalized dispersion coefficient vs laser fluence. Error bars are reported for each set of data

Karlsson et al. [27]. In their work, nephelometer scattering measurements and numerical simulation were performed on mini-CAST soot to retrieve information on particles morphology and the scattering wavelength dependence. In particular, they investigated the effect of morphology on the Scattering Ångström Exponent (SAE), which is a parameter mainly used in climate research models to express the scattering parameter wavelength dependence. They found that for soot aggregates small compared to the wavelengths under analysis (Rayleigh regime) the SAE is close to 4 and the wavelength dependence of the refractive index does not significantly affect the SAE. On the other hand, when the aggregates become comparable to the wavelength and the Mie theory comes into play, the SAE decrease down to 2. In our case, according to the particles size distributions reported in [6], pristine particles have a mean aerodynamic diameter of about 200 nm, thus falling in the case of rather big aggregates with dimension comparable to the wavelengths. Consequently, reduced SAE has to be considered. Instead laser-irradiated particles showed a significant reduction in the mean aerodynamic diameter and a strong increase in number density of very small particles already at 60 mJ cm^{-2}, suggesting aggregate fragmentation and/or the formation of small new particles. However, the volume distributions for the pristine and laser-irradiated particles look similar since they are dominated by the bigger particles. Therefore, recalling that the scattering cross section (ability of particles to scatter light) is proportional to the particle volume, it is reasonable to assume SAE equal to 2 also for the irradiated particles. However, it is worth stressing that this a first approximation and more work is needed to assess the scattering contribution in each of the experimental condition under investigation.

The evaluated scattering contribution is then subtracted to the extinction coefficient to retrieve the spectral behavior of the absorption coefficient, which is reported in Fig. 5. Data are normalized at the upper wavelengths (660–680 nm). An example of the scattering contribution for pristine particles is reported in Fig. S2 in the Supplementary Material.

Similarly to k_{ext}, the spectral behavior of k_{abs} changes already at the *LII peak* and then keeps evolving in few nanoseconds until it reaches the maximum modification in the final condition, when particles cooled down to ambient temperature.

To assess the impact of k_{abs} variation during laser-irradiation on LII data interpretation we took advantage of LII measurements previously performed on the same type of soot particles and published in Migliorini et al. [28], where LII prompt signals at 530 ($\Delta\lambda = 40$ nm) and 700 nm ($\Delta\lambda = 70$ nm) were collected as a function of the laser fluence. Here we evaluated the corresponding temperature

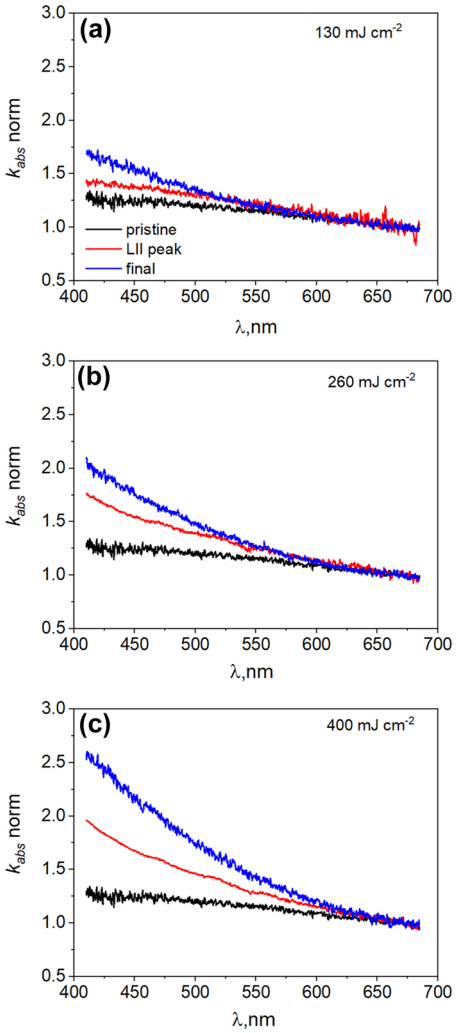

Fig. 5 Absorption coefficient spectral behavior of pristine and laser-irradiated particles for peak and final measurements at 130 mJ cm^{-2} (**a**), 260 mJ cm^{-2} (**b**), 400 mJ cm^{-2} (**c**). Data are normalized at the upper wavelengths (660–680 nm)

using either the absorption coefficient of pristine particles, thus assuming that laser-irradiation does not modify the particles optical properties, or k_{abs} at the *LII peak*. For clarity we report the expression used for temperature evaluation:

$$T = \frac{hc}{K_B}\left(\frac{1}{\lambda_2}-\frac{1}{\lambda_1}\right)\left[\ln\left(\frac{S_1 k_{abs(\lambda 2)}}{S_2 k_{abs(\lambda 1)}}\right)\left(\frac{\lambda_1}{\lambda_2}\right)^5\right]^{-1}, \qquad (3)$$

where S_1 and S_2 are the LII signals while $k_{abs(\lambda 1)}$ and $k_{abs(\lambda 2)}$ are the values of the absorption coefficient at 530 and 700 nm, respectively.

To this purpose, the k_{abs} curve shown in Fig. 5 are first extrapolated, using the corresponding dispersion coefficient, to retrieve the k_{abs} value at 700 nm. An example of the extrapolation procedure is reported in Fig. S3 in the

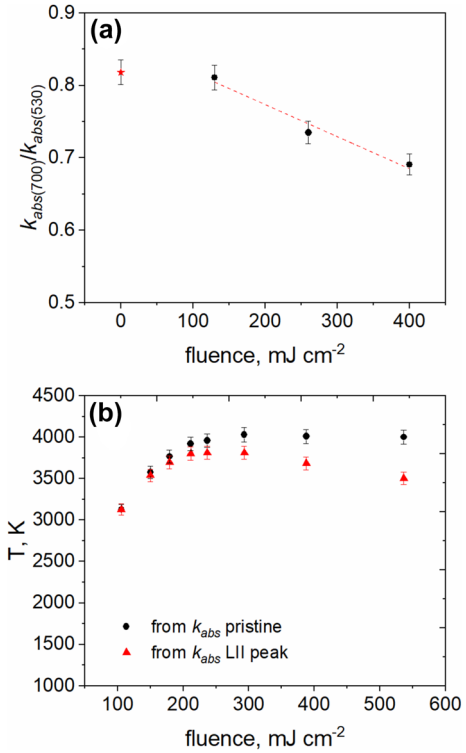

Fig. 6 $k_{abs(700)}/k_{abs(530)}$ ratio versus fluence (**a**) and temperature fluence curve (**b**) calculated using either k_{abs} of pristine particles or k_{abs} at the *LII peak*. Original LII data are from [28]. The red star in (**a**) represents the k_{abs} ratio of pristine particles

Supplementary Material. Then the ratio $k_{abs(700)}/k_{abs(530)}$ was evaluated for pristine and particles irradiated at 130, 260 and 400 mJ cm^{-2}, respectively. This ratio is found to remain constant for pristine and particles irradiated at 130 mJ cm^{-2} while decreases at 260 and 400 mJ cm^{-2}. Therefore, in this last fluence region, a linear interpolation is performed to estimate the k_{abs} ratio at the fluences used in [28]. The ratio $k_{abs(700)}/k_{abs(530)}$ and the linear fitting are reported in Fig. 6a while Fig. 6b shows the temperature curves. The corresponding uncertainties are also reported in the figure.

While in the low fluence regime the two curves are quite overlapped, an evident reduction in the incandescence temperature is observed for fluences above 200 mJ cm^{-2}. The decrease in the saturation temperature for irradiated mature soot particles was already observed in our recent work [17] and was ascribed to a shrinkage of particles due to fragmentation and/or vaporization with subsequent formation of new particles. Since particles temperature comes into play when evaluating soot volume fraction, particular attention has to be made if fluences higher than 200 mJ cm^{-2} are used for the measurement, at least for this type of soot particles.

For a deeper understanding of the change of the optical properties under laser irradiation, the time-evolution of

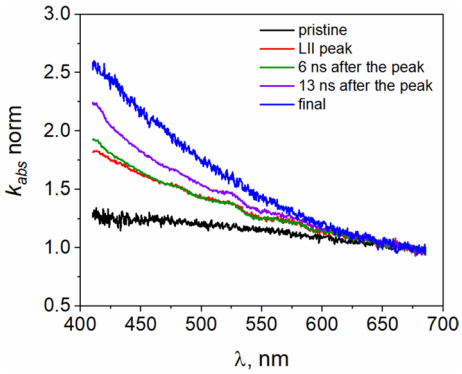

Fig. 7 Absorption coefficient time evolution of particles irradiated at 400 mJ cm^{-2}. Comparison with absorption coefficient of pristine nanoparticles. Data are normalized at the upper wavelengths (660–680 nm)

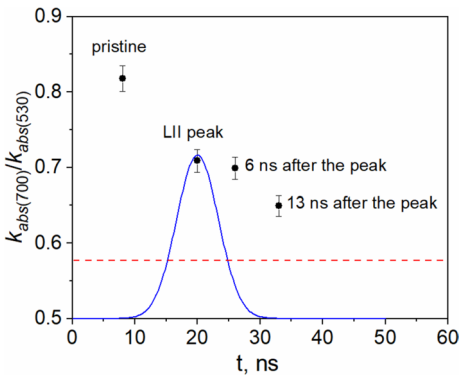

Fig. 8 k_{abs} ratio time evolution (symbols) with corresponding error bars. Laser pulse duration (blue line) and k_{abs} ratio value at the final condition measurement (dashed red line) are also reported

the absorption coefficient from the *LII peak* to the *final* condition is investigated at high laser fluence (400 mJ cm^{-2}) and reported in Fig. 7. Due to the short time-duration (about 30 ns) of the light source used for extinction measurement at the *LII peak* and the delay time between the spark and the occurrence of the incandescence peak (about 17 ns), it is not possible to investigate times longer than 13 ns after the LII peak.

After the initial variation from pristine to the LII peak condition, k_{abs} continues to change also during the first few nanoseconds after the peak. As a consequence, the ratio $k_{abs(700)}/k_{abs(530)}$ also changes during the first 13 ns after the LII peak as shown in Fig. 8. Here, the laser pulse duration is reported for comparison (blue curve) together with the k_{abs} ratio value at the final condition measurement, represented as an asymptotic red dashed line.

It is evident from Fig. 8 that a significant change in the particles optical properties happens within the laser pulse. This result might have strong implication in the application of time-resolved LII measurements for the determination of particle size. In fact, although this type of measurements is usually performed in the low fluence regime to avoid sublimation, it is not possible to exclude that the k_{abs} variation we observed at 400 mJ cm^{-2} occurs also at much lower fluences albeit to lesser extent.

Furthermore, such variation has to be taken into account when performing delayed or gated LII detection. The first one is usually performed in all the situations where the LII signal has to be discriminated against other signals, typically interference from C_2 and/or PHAs [1, 15]. The other one has been mostly used in LII imaging for spatially resolved visualization of particle distribution and/or concentration measurements in flames. In this case, it is common practice to use short gate widths on the order of 20–50 ns as a compromise between increasing the LII signal strength and reducing the interference from other emission as well the contribution from large particles to the LII signal. However, from our data, in this time frame the particles absorption properties already change significantly and therefore this variation needs to be taken into account.

Additionally, knowing the spectral behavior of the k_{abs} is of great advantage in the choice of LII detection wavelengths for particles temperature determination from pyrometry. In fact, considering that the absorption properties variation is more marked in the low wavelength region, the use of as short as possible lower detection wavelength and as long as possible upper detection wavelength (i.e. 400 and 700 nm), as suggested in the literature [29], might lead to a misinterpretation of the data. On the contrary, choosing two longer wavelengths might minimize the variation of the absorption properties, thus increasing the accuracy in particle temperature evaluation.

As a final remark, it is worth reminding that the effect of laser irradiation on soot absorption proprieties strongly depends on the nature of the particles, i.e. young or mature soot. Thus, the laser fluence threshold for particle properties modification may vary according to the efficiency of the heating process.

4 Conclusion

Wavelength-resolved extinction measurements on pristine and laser-irradiated mature soot particles were performed to investigate the effect of laser heating on soot optical properties. The experimental apparatus was properly designed to obtain the spectral behavior of soot optical properties during LII measurements, in correspondence with the LII prompt signal (*LII peak* condition), few nanoseconds after the LII peak and finally when the particles are in equilibrium with the surrounding environment (*final* condition). The results show that the absorption coefficient

already changes at the LII peak and the modification continues few nanoseconds after the peak until a permanent new condition is reached. The degree of the observed variation is strongly related to the laser energy density used. Further studies are required for a complete analysis and a deeper comprehension of the phenomena involved. In particular, particles size distributions after laser irradiation would help in improving the scattering contribution evaluation. Moreover, non-optical soot volume fraction measurements would be beneficial for the determination of the absolute value of the absorption coefficient before and after laser irradiation. Nevertheless, it is worth stressing the importance of our findings in relation to the impact of the absorption properties on the LII emission modelling. As far as, in particular working conditions, they change during laser irradiation, they strongly influence the experimental output. For this reasons it is suggested to control the effect of laser irradiation on soot absorption properties during LII measurements and to account for such phenomenon in LII data interpretation and/or in the evaluation of the uncertainties related to the measurements.

Supplementary Information The online version contains supplementary material available at https://doi.org/10.1007/s00340-023-08036-5.

Acknowledgements The authors would like to acknowledge the financial support from the PRIN Project 2017PJ5XXX: "Modeling and Analysis of carbon nanoparticles for innovative applications Generated dIrectly and Collected During combuSTion (MAGIC DUST)".

Author contributions FM: conceptualization, investigation, methodology, formal analysis, writing—original draft, and editing. RD: conceptualization, investigation, methodology, writing-review and editing. SD: conceptualization, methodology, writing-review and editing.

Data availability Data can be made available upon request to the authors for further exploration or use for model validation.

Declarations

Conflict of interest The authors declare no conflict of interest.

References

1. H.A. Michelsen, C. Schulz, G.J. Smallwood, S. Will, Laser-induced incandescence: particulate diagnostics for combustion, atmospheric, and industrial applications. Prog. Energy Combust. Sci. **51**, 2–48 (2015). https://doi.org/10.1016/j.pecs.2015.07.001
2. R.L. Vander Wal, M.Y. Choi, Pulsed laser heating of soot: morphological changes. Carbon **37**, 231–239 (1999). https://doi.org/10.1016/S0008-6223(98)00169-9
3. R.L. Vander-Wal, T.M. Ticich, A.B. Stephens, Optical and microscopy investigations of soot structure alterations by Laser—induced incandescence. Appl. Phys. B: Lasers Opt. **67**, 115–123 (1998). https://doi.org/10.1007/s003400050483
4. S. De Iuliis, F. Cignoli, S. Maffi, G. Zizak, Influence of the cumulative effects of multiple laser pulses on laser-induced incandescence signals from soot. Appl. Phys. B: Lasers Opt. **104**, 312–330 (2011). https://doi.org/10.1007/s00340-011-4535-y
5. H.A. Michelsen, A.V. Tivanski, M.K. Gilles, L.H. van Poppel, M.A. Dansson, P.R. Buseck, Particle formation from pulsed laser irradiation of soot aggregates studied with a scanning mobility particle sizer, a transmission electron microscope, and a scanning transmission X-ray microscope. Appl. Opt. **49**, 959–977 (2007). https://doi.org/10.1364/ao.46.000959
6. F. Migliorini, S. De Iuliis, R. Dondè, M. Commodo, P. Minutolo, A. D'Anna, Nanosecond laser irradiation of soot particles: insights on structure and optical proprieties. Exp. Therm Fluid Sci. **114**, 110064 (2020). https://doi.org/10.1016/j.expthermflusci.2020.110064
7. K.A. Thomson, K.-P. Geigle, M. Köhler, G.J. Smallwood, D.R. Snelling, Optical properties of pulsed laser heated soot. Appl. Phys. B: Lasers Opt. **104**, 307–319 (2011). https://doi.org/10.1007/s00340-011-4449-8
8. M. Saffaripour, K.-P. Geigle, D.R. Snelling, G.J. Smallwood, K.A. Thomson, Influence of rapid laser heating on the optical properties of in-flame soot. Appl. Phys. B: Lasers Opt. **119**, 621–642 (2015). https://doi.org/10.1007/s00340-015-6072-6
9. R.L. Vander Wal, K.A. Jensen, Laser-induced incandescence: excitation intensity. Appl. Opt. **37**, 1607–1616 (1998). https://doi.org/10.1364/AO.37.001607
10. P.O. Witze, S. Hochbreg, D. Kayes, H.A. Michelsen, C.R. Shaddix, Time-resolved laser-induced incandescence and laser elastic-scattering measurements in a propane diffusion flame. Appl. Opt. **40**, 2443–2452 (2001). https://doi.org/10.1364/ao.40.002443
11. H.A. Michelsen, P.E. Schrader, F. Goulay, Wavelength and temperature dependences of the absorption and scattering cross sections of soot. Carbon **48**, 2175–2191 (2010). https://doi.org/10.1016/j.carbon.2010.02.014
12. E. Therssen, Y. Bouvier, C. Schoemaecker-Moreau, X. Mercier, P. Desgroux, M. Ziskind, C. Focsa, Determination of the ratio of soot refractive index function $E(m)$ at the two wavelengths 532 and 1064 nm by laser induced incandescence. Appl. Phys. B: Lasers Opt. **89**(2), 417–427 (2007). https://doi.org/10.1007/s00340-007-2759-7
13. X. Lopez-Yglesias, P.E. Scrader, H.A. Michelsen, Soot maturity and absorption cross sections. J. Aerosol Sci. **75**, 43–64 (2014). https://doi.org/10.1016/j.jaerosci.2014.04.011
14. K.O. Johansson, F. El Gabaly, P.E. Schrader, M.F. Campbell, H.A. Michelsen, Evolution of particle surface and bulk maturity level during soot growth and oxidation in a flame. Aerosol Sci. Technol. **51**(12), 1333–1344 (2017). https://doi.org/10.1080/02786826.2017.1355047
15. S. Török, M. Mannazhi, P.-E. Bengtsson, Laser-induced incandescence (2λ and 2C) for estimating absorption efficiency

of differently matured soot. Appl. Phys. B: Lasers Opt. **127**(7), 96 (2021). https://doi.org/10.1007/s00340-021-07638-1
16. F. Migliorini, S. Belmuso, D. Ciniglia, R. Dondè, S. De Iuliis, A double pulse LII experiment on carbon nanoparticles: insight into optical properties. Phys. Chem. Chem. Phys. **24**, 19837 (2022). https://doi.org/10.1039/D2CP02639B
17. F. Migliorini, S. Belmuso, D. Ciniglia, R. Dondè, S. De Iuliis, Laser irradiation of different-aging carbon nanoparticles: study of the effect on optical properties. Appl. Phys. B: Lasers Opt. **1**, 1 (2023)
18. S. Török, M. Mannazhi, S. Bergqvist, K. Cuong Le, P.-E. Bengtsson, Influence of rapid laser heating on differently matured soot with double-pulse laser-induced incandescence. Aerosol Sci. Technol. **56**(6), 488 (2022). https://doi.org/10.1080/02786826.2022.2046689
19. S. De Iuliis, F. Migliorini, F. Cignoli, G. Zizak, Peak soot temperature in laser-induced incandescence measurements. Appl. Phys. B: Lasers Opt. **83**, 397–402 (2006). https://doi.org/10.1007/s00340-006-2210-5
20. A. Borghese, S.S. Merola, Time-resolved spectral and spatial description of laser-induced breakdown in air as a pulsed, bright, and broadband ultraviolet-visible light source. Appl. Opt. **37**, 3977–3983 (1998). https://doi.org/10.1364/AO.37.003977
21. F. Migliorini, K.A. Thomson, G.J. Smallwood, Investigation of optical properties of aging soot. Appl. Phys. B: Lasers Opt. **104**, 273–283 (2011). https://doi.org/10.1007/s00340-011-4396-4
22. J. Simonsson, N.E. Olofsson, S. Török, P.E. Bengtsson, H. Bladh, Wavelength dependence of extinction in sooting flat premixed flames in the visible and near-infrared regimes. Appl. Phys. B: Lasers Opt. **119**(4), 657–667 (2015). https://doi.org/10.1007/s00340-015-6079-z
23. C. Russo, B. Apicella, A. Tregrossi, A. Ciajolo, K. Cuong Le, S. Török, P.-E. Bengtsson, Optical band gap analysis of soot and organic carbon in premixed ethylene flames: comparison of in-situ and ex-situ absorption measurements. Carbon **158**, 89–96 (2020). https://doi.org/10.1016/j.carbon.2019.11.087
24. F. Migliorini, S. Belmuso, R. Dondè, S. De Iuliis, In-flow optical characterization of flame-generated carbon nanoparticles sampled from a premixed flame. Phys. Chem. Chem. Phys. **23**, 15702–15712 (2021). https://doi.org/10.1039/d1cp01267c
25. R.C. Millikan, Optical properties of soot. J. Opt. Soc. Am. **51**, 698–699 (1961). https://doi.org/10.1364/JOSA.51.000698
26. P. Minutolo, G. Gambi, A. D'Alessio, The optical band gap model in the interpretation of the UV–visible absorption spectra of rich premixed flames. Proc. Combust. Inst **26**, 951–967 (1996). https://doi.org/10.1016/S0082-0784(96)80307-9
27. A. Karlsson, S. Török, A. Roth, P.-E. Bengtsson, Numerical scattering simulations for estimating soot aggregate morphology from nephelometer scattering measurements. J. Aerosol Sci. **159**, 10528 (2022). https://doi.org/10.1016/j.jaerosci.2021.105828
28. F. Migliorini, S. De Iuliis, S. Maffi, G. Zizak, Saturation curves of two-color laser-induced incandescence measurements for the investigation of soot optical properties. Appl. Phys. B: Lasers Opt. **120**, 417–427 (2015). https://doi.org/10.1007/s00340-015-6151-8
29. F. Liu, D.R. Snelling, K.A. Thomson, G.J. Smallwood, Sensitivity and relative error analyses of soot temperature and volume fraction determined by two-color LII. Appl. Phys. B: Lasers Opt. **96**, 623–636 (2009)